analytical chemistry

pubs.acs.org/ac Article

Using the Quartz Crystal Microbalance to Monitor the Curing of Drying Oils

Gwen dePolo, Arnaud Lesaine, Marco Faustini, Lucie Laporte, Côme Thillaye du Boullay, Étienne Barthel, Joen Hermans, Piet D. Iedema, Laurence de Viguerie,* and Kenneth R. Shull*

Cite This: *Anal. Chem.* 2024, 96, 10551−10558 Read Online

ACCESS | Metrics & More | Article Recommendations | Supporting Information

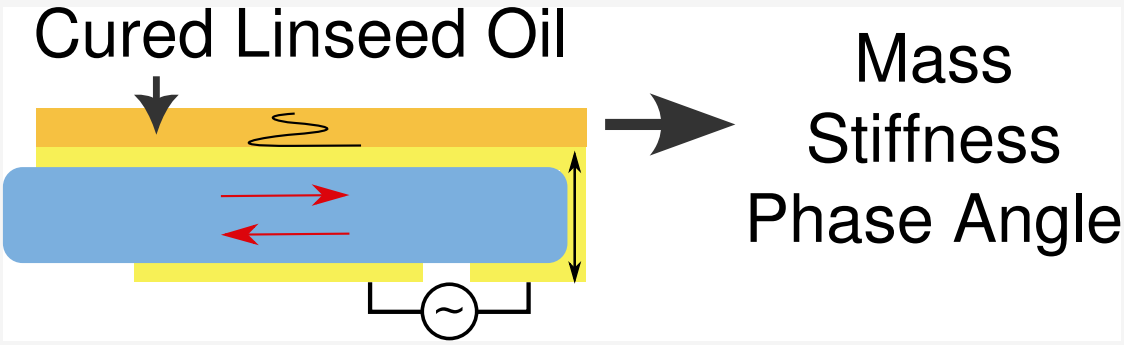

ABSTRACT: Drying oils such as linseed oil form a polymer network through a complex free-radical polymerization process. We have studied polymerization in this challenging class of polymers using a quartz crystal microbalance (QCM). The QCM is able to measure the evolution of polymer mass and mechanical properties as the oil transitions from a liquid-like to a solid-like state. Measurements using bulk materials and thin films provide information about the initial polymerization phase as well as the evolution of the mass and mechanical properties over the first two years of cure. The temperature-dependent response of the cured linseed oil films was also measured. These results were combined with previously published results obtained from traditional dynamic mechanical analysis to give a unified picture of the properties of these materials across a very broad temperature range.

INTRODUCTION

Since the 15th century, linseed oil has been commonly used by painters as a binding medium for paints.[1] One of the material properties that drew painters to using linseed oil was its ability to mix with pigments and additives, coat surfaces well, and then undergo a curing process to form a solid film. To speed up this process, it was common practice to treat the oil before using it, in particular by heating in the presence of siccatives (usually lead compounds).[2,3] In drying oils such as linseed oil, a polymer film forms as a result of an auto-oxidation process where peroxide, ether, and alkyl cross-links are formed as a result of oxygen reacting with unsaturated fatty acid chains in triglyceride molecules of the oil.[4−6] While there are many chemical reactions that contribute to the curing process of drying oils, on a more macroscopic level, the oil will transition from being liquid-like to solid-like as the polymer film forms. The stiffness of a polymer system increases as cross-links form between polymer chains. Cross-link formation in drying oils is typically considered a slow curing process, while most synthetic polymer systems use ultraviolet light, temperature, or chemical initiators to induce and accelerate this process.[7−10] It is important to learn how drying oils form networks in order to ultimately understand long-term degradation and the factors that influence network stability.[11−14] The network formation process of linseed oil has been studied extensively through chemical investigations including infrared spectroscopy and chromatographic analysis,[2,3,12,15,16] but the mechanical properties during the initial curing step have never been properly characterized. The sol−gel transition associated with polymer network formation makes the most common approaches to measuring the mechanical properties of this film impractical to use. Rheology is most ideally used on liquid-like samples and has been used to understand the flow and application properties of paints and drying oils with an emphasis on the effects of historic preparation recipes for these oils.[17−21] Tensile testing, dynamic mechanical analysis (DMA), and micro/nano-indentation can be used to investigate the mechanical properties of dried films, but the samples must be solid in order to be measured, making

Received: February 19, 2024
Revised: May 20, 2024
Accepted: May 20, 2024
Published: June 18, 2024

https://doi.org/10.1021/acs.analchem.4c00938
Anal. Chem. 2024, 96, 10551−10558

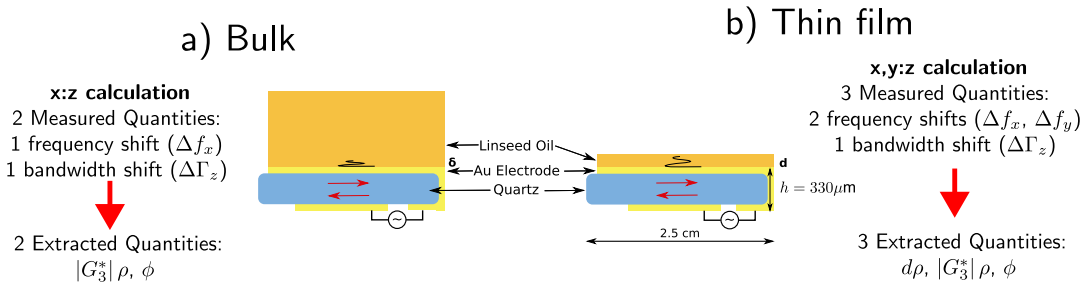

Figure 1. (a) Bulk and (b) thin-film sample geometries used for experiments with the QCM in this study. The quartz crystal sample substrate consists of a quartz disk (thickness of 330 μm and a diameter of 2.5 cm) with two gold (Au) electrodes on either surface.

these techniques not feasible to use on oil films that have not reached an initial state of cure.[11,22−31]

The quartz crystal microbalance (QCM) is a uniquely suitable technique to measure the mechanical properties of a polymer film experiencing a liquid to solid transition. This technique uses the piezoelectric properties of quartz to propagate a mechanical shear wave at high frequencies (MHz) through a film of interest, as illustrated in Figure 1.[32,33] The resulting shifts in the resonant frequencies of the quartz crystal can be used to determine the mass and mechanical properties of the film.[34] A QCM sample typically has a surface of the film open to the surrounding environment, which can make it an ideal technique for looking at changes in the mechanical properties as a result of temperature, relative humidity, or exposure to solvent.[9,35−38] The films of interest are also fairly thin (on the order of 0.7−6 μm), effectively removing any diffusion barrier that would be present for a bulk film. The QCM has been previously used to characterize the evolution of mechanical properties in many polymer systems, including an alkyd binding medium, which undergoes a similar curing mechanism to that of linseed oil.[9,34−36,38−45] In the present work, we use linseed oil as a case study to illustrate both the strengths and limitations of the use of the QCM to investigate time-dependent physical property changes for times ranging from minutes to years.

The detailed mathematical formulation that relates the measured QCM response to the properties of the thin film has been discussed previously[34,46,47] and is included in the Supporting Information for completeness. Briefly, we measure the resonant frequency and bandwidth (equivalent to the dissipation that is often reported in experiments referred to as QCM-D experiments) at multiple harmonics of the crystal resonance, both before and after a thin film of material is deposited on the electrode surface of the QCM. In the most general "thin film" analysis illustrated in Figure 1b, three quantities related to the behavior of the crystal resonances are obtained and the following three film properties are extracted.

- dρ, the product of the film thickness and density, or equivalently, the mass per unit area of the film.
- $|G_3^*|\rho$, the product of the density and magnitude of the complex shear modulus at the third resonant harmonic (15 MHz in our case).
- ϕ, the viscolastic phase angle, assumed to be the same for the different harmonics that are used. This quantity is more commonly referred to as δ in the rheological community, but we use ϕ here to remain consistent with our previous work and to distinguish it from the decay length, defined below in eq 1.

In the simpler bulk analysis shown in Figure 1a, we measure two quantities (typically the resonant frequency shift and bandwidth at the third harmonic) to obtain $|G_3^*|\rho$ and ϕ, obtaining no information about the total mass of the sample.

In the current paper, we use the QCM to address the following questions as they pertain to linseed oil.

- How do the viscoelastic properties of linseed oil evolve during the very early stages of the curing process?
- How does an oil pretreatment (heating in the presence of lead oxide, commonly reported in historic recipes) affect the curing kinetics and the mechanical properties of the fully cured systems?
- What is the temperature dependence of the mechanical properties of oil films dried in different conditions? We are particularly interested in identifying the glass transition temperature, T_g, where the material behavior transitions from rigid, glassy behavior (below T_g) to soft, rubbery behavior (above T_g).

We also address a series of more general, practical issues pertaining to the use of QCM to determine the mechanical properties of materials. These issues include the limitations of the relatively simple bulk analysis, the optimized sample thicknesses and harmonics to be used for a QCM measurement, and a quantitative uncertainty analysis of the mechanical properties that are obtained.

MATERIALS AND METHODS

Three different types of linseed oil were used in this study, which we refer to as SA, KP, and WN, based on the supplier.

- SA: boiled linseed oil from Sigma-Aldrich (without siccative)
- KP: cold-pressed linseed oil from Kremer Pigmente, also used by Baij et al. in their previously reported DMA experiments[48]
- WN: refined linseed oil from Winsor & Newton

To better understand the influence of oil pretreatment, we prepared oil according to historical recipes[3] by heating it with PbO. Litharge (PbO) was purchased from Sigma-Aldrich and mixed with the KP cold-pressed linseed oil to give samples with PbO weight fractions of 0.05 and 0.2. These samples were prepared by placing the PbO into a mortar and grinding with a few drops of oil. The rest of the oil was added to this PbO paste in a beaker and heated at 150 °C for 2 h under magnetic stirring. The linseed oils from Sigma-Aldrich and Winsor & Newton were used as is. As preparation layers for the substrate, either polystyrene (192k MW, Sigma-Aldrich) or 1-propanethiol was used. Toluene, turpentine, mineral spirits, and tetrahydrofuran were used as solvents during the spin-casting for the pretreatment and oil films. The oils were cast on quartz crystal electrodes (AT-cut, 2.54 cm diameter, 330 μm thickness) purchased from

https://doi.org/10.1021/acs.analchem.4c00938
Anal. Chem. 2024, 96, 10551−10558

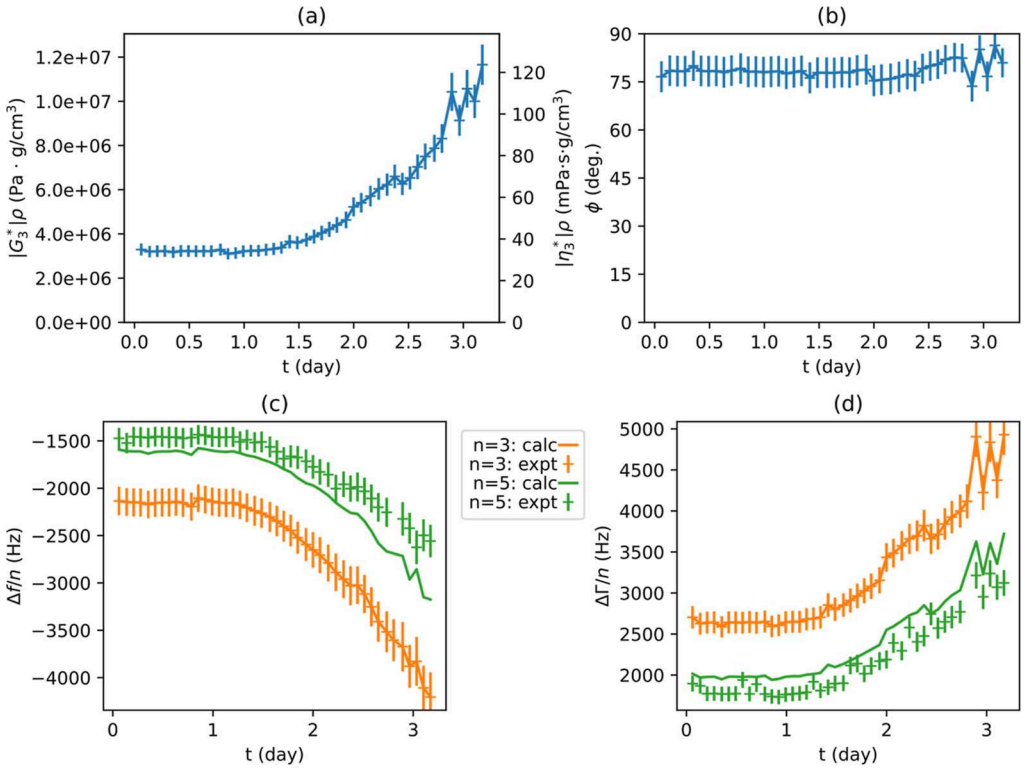

Figure 2. Measured time-dependent properties (a,b) and solution checks (c,d) for the bulk SA linseed oil sample. The solution checks compare the experimentally measured values of Δf_n and $\Delta\Gamma_n$ to the values of these quantities that are calculated from the measured properties. Because this is a 3:3 calculation, properties are determined from the requirement that experimental and calculated values are in agreement for Δf_3 and $\Delta\Gamma_3$. Uncertainties in Δf_n and $\Delta\Gamma_n$ are slightly larger than 5% of $\Delta\Gamma_n$ and are used to determine uncertainties in the measured properties as described in the Supporting Information.

Table 1. Extracted Physical Properties of the SA Bulk Sample at Early and Late Stages of Drying[a]

	$\lvert G_3^*\rvert\rho$ (Pa g/cm^3)	ϕ (deg)	ρ (g/cm^3)	δ_3 (μm)	$\lvert\eta_3^*\rvert$ (mPa·s)	$\Delta\Gamma_3$ (Hz)
water	9.4×10^4	90	1	0.145	1	1230
linseed oil, t = 1 h	3.5×10^6	80	0.93	1.05	40	8160
linseed oil, t = 72 h	1.1×10^7	80	0.93	1.86	125	14,500

[a]Measurements are no longer possible when the bandwidth, Γ, is larger than ≈20 kHz.

Renlux (Nanshan, China) and Advanced Wave Sensors (AWS, Valencia, Spain). Additional details of the sample preparation, including substrate pretreatments used to minimize complications arising from potential dewetting of the thin linseed oil film, are included in the Supporting Information.

RESULTS

Bulk Analysis of Early Stage Cure. A bulk sample of the SA linseed oil was measured to determine the initial viscosity, the change in mechanical properties over time, and the extent to which those changes could be observed by using this experimental geometry. Values of $\lvert G_3^*\rvert\rho$ (or equivalently, $\lvert\eta_3^*\rvert\rho$ where $\lvert\eta_3^*\rvert$ is the magnitude of the complex shear viscosity at the third harmonic frequency) and ϕ are plotted in Figure 2. Assuming a density of 0.93 g/cm^3 for linseed oil, we obtain the magnitude of the complex viscosity as it increases from 40 mPa·s at the beginning of the experiment to 125 mPa·s after about 3 days. The initial value is consistent with the viscosity of 44 mPa·s determined from rheological steady state flow experiments at shear rates of 0.01−100 s^{-1}, see the Supporting Information), which are much lower than the angular frequency of ≈10^8 s^{-1} for the QCM experiments. The properties remained constant for the first 1.5 days. This initial period of constant viscosity is attributed to the presence of antioxidants in the linseed oil, which react with oxygen before the auto-oxidation process begins. Auto-oxidation induces cross-link formation in the oil and increases the complex shear modulus/viscosity as well as the decay length.

The QCM senses the properties of the material in the immediate vicinity of the electrode surface within a distance determined by the decay length, δ, of the shear wave in the oil, which is determined by the frequency and the viscoelastic properties of the material

$$\delta = \frac{(\lvert G^*\rvert/\rho)^{1/2}}{2\pi f \sin(\phi/2)} \quad (1)$$

When the viscosity in this portion of the sample becomes sufficiently large, the sample moves from the "bulk" regime (where the sample thickness, d, is assumed to be much larger than δ) to the "overdamped" regime and quantitative measurements are no longer possible.[44] Table 1 provides the decay length for water (a Newtonian liquid) as well as the SA bulk sample at early and later times of cure along with the mechanical

https://doi.org/10.1021/acs.analchem.4c00938
Anal. Chem. 2024, 96, 10551−10558

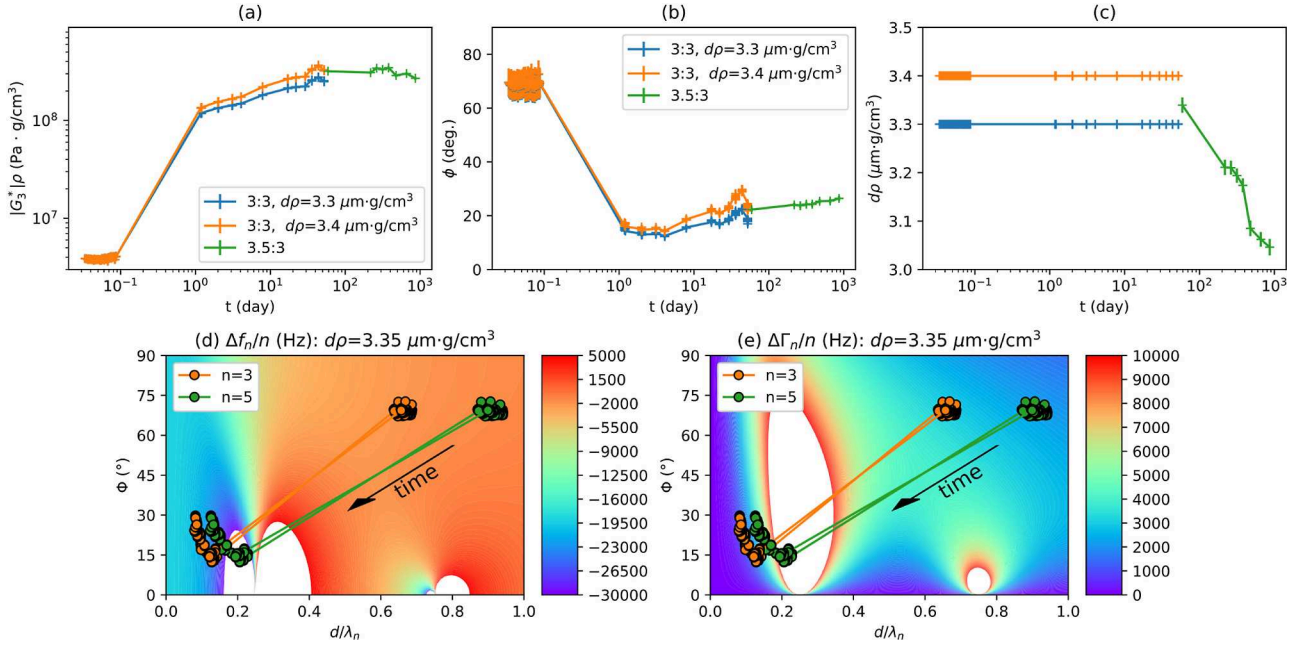

Figure 3. Evolution of mechanical properties over time of the SA sample. The extracted properties ($|G_3^*|\rho$, ϕ, and dρ) are shown in (a–c). The 3:3 calculations use only the 3rd harmonic, assuming a fixed value of dρ listed in the legend. A 3.5:3 calculation was used for later times (t > 55 days). Response maps for the SA LO sample are shown in (d,e). The color maps correspond to values of $\Delta f/n$ and $\Delta\Gamma/n$ calculated with the assumption that dρ = 3.35 μm·g/cm^3. This value of dρ is representative of the values obtained throughout the experiment. The specific choice of dρ here affects the detailed visualization of the response map, but it does not affect the analysis itself.

properties obtained from the QCM experiment. The most important outcome from these bulk experiments is the conclusion that they are restricted to materials with complex moduli below ≈2 × 10^7 Pa. This result is consistent with the range of moduli for which this same bulk analysis has been used by Szántó et al. in their QCM measurements of the rheological properties of polyethylene and copolymers of ethylene/vinyl acetate.[49] For larger values of $|G^*|$, Γ is too large to give a well-defined resonance, as described in more detail in the Supporting Information. For liquid samples at our measurement frequency of 1.5 × 10^7 Hz, this limitation restricts us to materials with viscosities less than ≈0.2 Pa·s, which is 200 times the room-temperature viscosity of water. This limitation is rather severe in the context of studying polymerization processes and motivates the development of the more complicated thin-film analysis utilized in the following section.

Thin-Film Analysis. *Film Thickness Considerations.* Two linseed oils processed in different ways, SA and WN, were measured in ambient lab conditions, and the evolution of mechanical properties was followed. Results obtained from the SA oil sample are particularly useful for illustrating the importance of the sample thickness. For this sample, two complementary analysis approaches were used to obtain the properties shown in Figure 3a–c. For the longer aging times (t < 55 days), the dissipation for the fifth harmonic is low enough so that a suitably accurate value of Δf_5 is obtained. In these cases, the properties were obtained from a 3.5:3 calculation, where values of Δf_3, Δf_5, and $\Delta\Gamma_3$ are used. For shorter aging times, the dissipation for the fifth harmonic is too large, meaning that Δf_5 cannot be accurately measured. In this case, we used a 3:3 calculation involving only Δf_3 and $\Delta\Gamma_3$, assuming values of dρ determined from the longer aging times. We use two values of dρ that bracket the 55 day value obtained from the 3.5:3 calculation, and they differ from one another by 3%. In this way, we assess the sensitivity of the extracted properties to this assumed thickness. As shown in Figure 3, the assumed value of dρ has a negligible effect on the measured values of $|G_3^*|\rho$ and ϕ at the shortest aging times. At the larger aging times, a 3% deviation in the assumed value of dρ results in a 25% deviation in the calculated values of $|G_3^*|\rho$ and ϕ.

The inability to measure film properties for intermediate aging times can be understood in terms of the response maps for these data shown in Figure 3d,e. An important parameter here is λ_n, the wavelength of the shear wave in the viscoelastic medium, which is related to the frequency and viscoelastic properties of the film as follows[34]

$$\lambda_n = \frac{1}{f_n}\left(\frac{|G_n^*|}{\rho}\right)^{1/2}\frac{1}{\cos(\phi/2)} \tag{2}$$

Here, we include the harmonic number n as a reminder that we are collecting data at multiple frequencies, accounting for a frequency dependence of G_n^* but assuming that ϕ is independent of n for the values of n that are used in the calculation of the properties. We further assume that $|G_n^*|$ increases with frequency (or n), according to the following power law

$$|G_n^*| \propto \phi^{n/90} \tag{3}$$

with ϕ in degrees. Equation 3 becomes exact, with a frequency-independent phase angle, if the power law is valid over a very wide frequency range above and below the frequencies of interest,[50,51] but is in general an approximation. This approximation is surprisingly good, standardizing and simplifying the analysis while introducing an error that remains small in comparison to errors originating from experimental uncertainties in the measured values of Δf and $\Delta\Gamma$. For example, it was previously shown using typical experimental data for a cross-

https://doi.org/10.1021/acs.analchem.4c00938
Anal. Chem. 2024, 96, 10551−10558

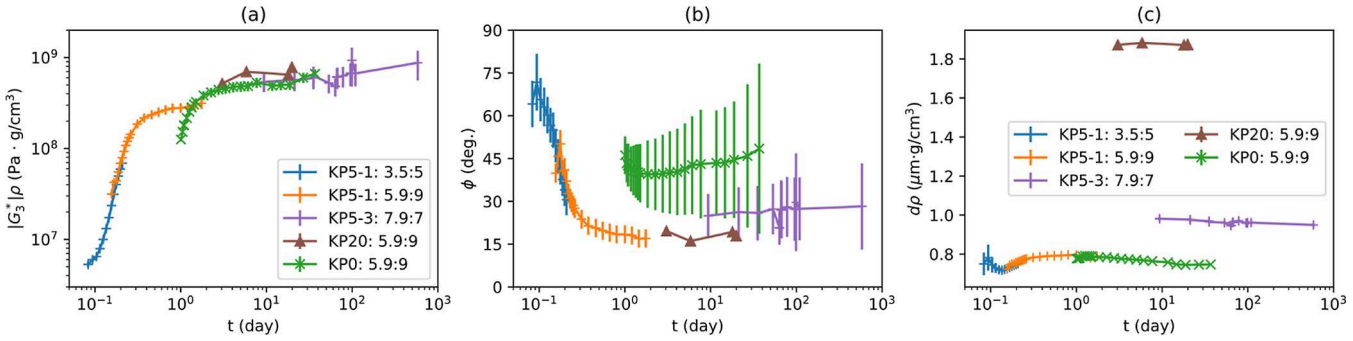

Figure 4. Evolution of $|G_3^*|\rho$ (a), ϕ (b), and dρ (c) for the KP films with no added PbO (KP0), with 5 wt % PbO (KP5−1 and KP5−3) and 20 wt % PbO (KP20). The legend for (b) is identical to the legends for (a,c).

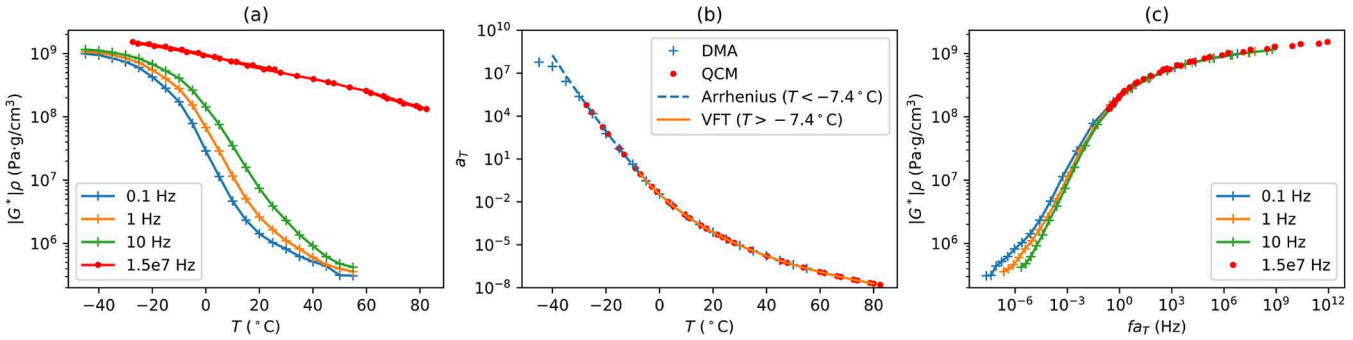

Figure 5. (a) Temperature dependence of $|G^*|\rho$ at 1.5×10^7 Hz from the QCM data and at much lower frequencies from the DMA data from Baij et al.[48] (b) Temperature-dependent shift factors with an Arrhenius fit (eq 6, E_a = 300 kJ/mol) for temperatures less than −7.4 °C and a Vogel−Fulcher−Tammann fit (eqs 7) for temperatures above −7.4°. (c) Master curve for $|G^*|\rho$ using the temperature shift factors from part (b).

linked polymer that in the regime where the thin-film analysis is necessary ($|G^*| \gtrsim 2 \times 10^7$ Pa); this constant phase angle approximation introduces an error no larger than 10% in the measured values of both ϕ and $|G^*|\rho$.[47]

Response maps are a graphical representation of the following QCM master equation for the thin-film regime[34]

$$\Delta f_n^* \equiv \Delta f_n + i\Delta\Gamma_n = -\Delta f_{sn}\left(\frac{\tan\{(2\pi d/\lambda_n)(1 - i\tan(\phi_n/2))\}}{(2\pi d/\lambda_n)(1 - i\tan(\phi_n/2))}\right) \quad (4)$$

Here, Δf_{sn} is the Sauerbrey frequency shift

$$\Delta f_{sn} = \frac{2nf_1^2}{Z_q}\rho d \quad (5)$$

where Z_q is the acoustic impedance of quartz (8.84×10^6 kg/m^{2}s for the AT quartz used here).

For this sample, the early times are in the upper right corner with high d/λ_n (equivalent to a lower complex shear modulus) and a high phase angle. As the sample polymerizes over a period of several hours, the data shift to the lower left corner of the response maps. The areas of white on the response maps are where the film resonance phenomenon occurs, giving values for Γ that are too large for mechanical property data to be obtained. In order for this region to be avoided so that data can be obtained throughout the entire curing process of the same sample, thinner samples must be used, as is the case for the remainder of the samples discussed in this paper.

Effect of Oil Treatment with PbO. The next comparison we investigated involved the addition of PbO to linseed oil, a common technique used by painters throughout history to reduce the drying time of the oil paints and improve the properties for paint application to a surface.[3,52−54] This treatment leads to partial saponification of the oil (among other reactions due to heating). For these measurements, cold-pressed linseed oil (KP) was chosen. The time-dependent properties of the KP films are summarized in Figure 4 and involve the following samples.

- One film without PbO (KP0) that was monitored over 4 days.
- Three films of oil +5% PbO (KP5−1,2,3) that were monitored for periods ranging from 1 h to two years.
- One film of oil +20% PbO (KP20) that was monitored from 3 days to 3 weeks.

Property uncertainties become large for the thinnest films, where d/λ_n becomes too small to determine accurate properties to be determined. Property uncertainties for the KP5−2 film are particularly large, and data from this film are not included in Figure 4 for this reason. Solution checks and response maps for each of the samples are included in the Supporting Information.

Two of the KP samples capture the evolution of the mechanical properties during the initial polymerization of the film: KP0 and KP5−1, where $|G_3^*|\rho$ increases and ϕ decreases. These changes in the mechanical properties are due to oxygen uptake by the film, which fuels the autoxidative polymerization of the films. The main difference between these two films is the time at which this polymerization occurred, at approximately 25 and 3−5 h for the KP0 and KP5−1 films, respectively. This difference in the rate of initial polymerization is a result of using PbO as a siccative and as part of a heat treatment for the linseed oil. To fully capture this initial polymerization regime for the

https://doi.org/10.1021/acs.analchem.4c00938
Anal. Chem. 2024, 96, 10551−10558

KP5−1 sample, two different calculations were used, 3.5:5 for times less than 4.5 h and 5.9:9 for longer times. A detailed comparison of these two calculations is included in the Supporting Information.

One important result from these samples is the similarity of $|G_3^*|\rho$ at times greater than 4 days for all the samples. These moduli are comparable to the values obtained for oil paints measured using tensile testing as well as well as the values determined by the QCM for a commercial alkyd binding medium.[22,23,36] Note that because of the high frequency of the QCM measurement (15 MHz), this technique accesses the glassy regime of the cured films, even at temperatures above the glass transition temperature. We expand on this point below in the section on the effects of the temperature on the mechanical properties.

Temperature-Dependent Mechanical Properties of Cured Oil Films. The WN film was of sufficient quality so that temperature sweeps could be performed from −40 to 80 °C. Results from the QCM measurements after room temperature aging at 5 months are shown in Figure 5a. Also included in this plot are published data from Baij et al. for linseed oil films that were cured overnight at 150 °C.[48] Measured values of E^* (the complex dynamic modulus in extension) from Baij et al. were converted to values of $G^*\rho$ as described in the Supporting Information. In addition to the different processing conditions (long-term cure at room temperature vs shorter cure at 150 °C) and linseed oil source (KP vs WN), an important difference between our measurements and those of Baij et al. concerns the frequency of our measurements. The measurements of Baij et al. were performed at frequencies of 0.1, 1, and 10 Hz, whereas our QCM data correspond to a measurement frequency of 1.5×10^7 Hz. Comparison of the data obtained at these very different frequencies requires the use of time−temperature superposition, where the frequencies are multiplied by the temperature-dependent shift factors, a_T. These shift factors are determined by the requirement that superposable master curves be obtained when the viscoelastic properties are plotted as a function of the reduced frequency, fa_T. These shift factors are important in that they describe the temperature dependence of the mechanical relaxation times within the material.

The shift factors generated from our analysis of the data are shown in Figure 5b. The corresponding rheological master curves, where we plot $|G^*|\rho$ as a function of the temperature-shifted frequency (fa_T) for all of the data, are shown in Figure 5c. An important parameter here is the glass transition temperature, T_g. Several different metrics can be applied to specify the T_g for viscoelastic materials. Use of the maximum in the phase angle at a specified frequency (typically 1 Hz) is one example, which in this case gives $T_g \approx 8$ °C.[48] In synthetic polymers, the onset of material softening at 1 Hz as the sample is heated is more closely correlated with the calorimetrically determined glass transition temperature.[43] With this criterion (described more quantitatively in the Supporting Information), we obtain $T_g \approx -7.4$ °C for these materials. This is the value of T_g that we assume in the remainder of our discussion.

Below T_g, the low-frequency DMA results from Baij et al. are best suited for determination of the shift factors, whereas the QCM results are needed to obtain shift factors at higher temperatures. For temperatures between −35 °C and T_g, the shift factors obey an Arrhenius temperature dependence, with a_T given by the following

$$\ln a_T = \frac{E_a}{RT} - \frac{E_a}{RT_{ref}} \tag{6}$$

Here, R is the gas constant, T is the absolute temperature, E_a is the activation energy, and T_{ref} is an arbitrarily defined reference temperature, for which we use T_g (−7.4 °C). The dashed curve in Figure 5b is a representation of eq 6, with an E_a = 300 J/mol. This Arrhenius temperature dependence for segmental relaxation processes below T_g, and the specific value of E_a that we obtain, is consistent with results obtained for other synthetic polymers.[55]

At temperatures above T_g, the temperature shift factors obey the Vogel−Fulcher−Tamaan (VFT) form

$$\ln a_T = \frac{B}{T - T_\infty} - \frac{B}{T_{ref} - T_\infty} \tag{7}$$

We handle the crossover between the Arrhenius and VFT forms at $T = T_g$ by requiring that $d \ln a_T/dT$ be continuous at T_g, so that B is related to E_a in the following manner

$$B = \frac{E_a}{R}\left(\frac{T_g - T_\infty}{T_g}\right)^2 \tag{8}$$

We use T_∞ as the remaining adjustable parameter to force agreement between the high-frequency QCM data and the low-frequency DMA data. As shown in Figure 5b, excellent agreement between the DMA and QCM data are obtained if T_∞ = −65 °C, which from eq 8 gives B = 1700 K. This value for T_∞ is consistent with results obtained for a wide variety of polymers, where T_∞ is found to be about 50 K below T_g.[55] Overall, we find that by combining results obtained with traditional dynamic mechanical analysis with our QCM results, an accurate set of shift factors are obtained from −45 to 85 °C.

While the analysis presented above does not necessarily prove the similarity of properties for linseed oil aged under very different conditions, the internal consistency of the analysis is compelling evidence for the similarity of the properties in the glass transition regime ($G > 10^8$ Pa) where data are obtained from both the DMA and QCM experiments. However, it is important to keep in mind that this similarity is restricted to the glassy and near-glassy regimes. Because of limitations imposed by the very high frequency, the QCM is only able to access the material behavior in the behavior of cured linseed oil in the regime where the modulus is greater than 10^8 Pa. The detailed degree of cross-linking and overall network topology affect the relaxed, rubbery modulus at values of fa_T that are too low to be accessed by the QCM, even at elevated temperatures. While the glassy dynamics of the different linseed oil samples cured at very different temperatures appears to be quite similar, it is entirely possible that the network architectures of the two samples differ in more substantial ways.

CONCLUSIONS

The QCM can be utilized to track curing and aging processes of thin films as they are exposed to the ambient environment. In this work, we have demonstrated the capability with linseed oil films that are of significant interest to the conservation science community. Two types of analyses were performed. The "bulk" analysis is the most easily employed and requires that accurate measurements be obtained for a single crystal resonance, in our case the third harmonic at a frequency of 15 MHz. This analysis can be utilized when the magnitude of the complex shear

https://doi.org/10.1021/acs.analchem.4c00938
Anal. Chem. 2024, 96, 10551−10558

modulus at 15 MHz is less than about 2×10^7 Pa, corresponding to a complex viscosity of about 200 mPa·s (200 times the viscosity of water). This limitation is a substantial one, and more complicated "thin film" analysis must be utilized in most cases. Data from two different harmonics are generally required, and the film thickness must also be in a relatively narrow range, typically near 1 μm for the linseed oil films investigated here. By working with a film of the appropriate thickness and choosing the most appropriate harmonics for the analysis, it is possible to obtain data from the uncured to fully cured states from the same film. A useful general guideline for the analysis is that the thickness of the film should be from 5 to 15% of the wavelength of the shear wave at the harmonics utilized, although useful data outside this range can sometimes be utilized. Also, when the film mass can be assumed to be constant (as with a temperature-dependent study, for example), data from a single harmonic are sufficient, providing access to a broader range of material properties. With regard to the linseed oil samples investigated here, we showed that the addition of PbO accelerates the cure kinetics by a factor of 5. Also, we showed that the glassy polymer dynamics obtained from the QCM are consistent with properties obtained from similar linseed oil films with traditional dynamic mechanical analysis at frequencies from 0.1 to 10 Hz. Addition of the QCM data obtained at 15 MHz to this previous data set enables us to accurately measure the temperature dependence of the polymer relaxation times (quantified by the temperature shift factors a_T) to much higher temperatures than can be accomplished with the DMA data alone.

■ ASSOCIATED CONTENT

Supporting Information

The Supporting Information is available free of charge at https://pubs.acs.org/doi/10.1021/acs.analchem.4c00938.

QCM theory and sample regimes, sample preparation and measurements, comparison of QCM calculation methods, ellipsometric measurements, bulk rheological measurements, solution checks and response maps for KP thin films, analysis of temperature-dependent properties, generalized power law model and T_g determination, and reflection Fourier transform infrared spectroscopy measurements (PDF)

■ AUTHOR INFORMATION

Corresponding Authors

Laurence de Viguerie − *Laboratoire d'Archéologie Moléculaire et Structurale (LAMS), CNRS UMR 8220, Sorbonne Université, 75005 Paris, France;* orcid.org/0000-0002-7038-6979; Email: laurence.de_viguerie@sorbonne-universite.fr

Kenneth R. Shull − *Department of Materials Science and Engineering, Northwestern University, Evanston, Illinois 60208, United States;* orcid.org/0000-0002-8027-900X; Email: k-shull@northwestern.edu

Authors

Gwen dePolo − *Department of Materials Science and Engineering, Northwestern University, Evanston, Illinois 60208, United States; Van't Hoff Institute for Molecular Sciences, University of Amsterdam, Amsterdam, The Netherlands;* orcid.org/0000-0002-2103-1231

Arnaud Lesaine − *Laboratoire d'Archéologie Moléculaire et Structurale (LAMS), CNRS UMR 8220, Sorbonne Université, 75005 Paris, France; Laboratoire Chimie de la Matière Condensée de Paris LCMCP, CNRS, Sorbonne Université, 75005 Paris, France*

Marco Faustini − *Laboratoire d'Archéologie Moléculaire et Structurale (LAMS), CNRS UMR 8220, Sorbonne Université, 75005 Paris, France; Laboratoire Chimie de la Matière Condensée de Paris LCMCP, CNRS, Sorbonne Université, 75005 Paris, France;* orcid.org/0000-0002-6254-5116

Lucie Laporte − *Laboratoire d'Archéologie Moléculaire et Structurale (LAMS), CNRS UMR 8220, Sorbonne Université, 75005 Paris, France*

Côme Thillaye du Boullay − *Laboratoire d'Archéologie Moléculaire et Structurale (LAMS), CNRS UMR 8220, Sorbonne Université, 75005 Paris, France*

Étienne Barthel − *Soft Matter Sciences and Engineering, ESPCI Paris, PSL University, CNRS, Sorbonne Université, 75005 Paris, France*

Joen Hermans − *Van't Hoff Institute for Molecular Sciences, University of Amsterdam, Amsterdam, The Netherlands; Conservation & Science, Rijksmuseum, Amsterdam, The Netherlands; Conservation & Restoration, Amsterdam School of Heritage, Memory and Material Culture, University of Amsterdam, Amsterdam 1012 WP, The Netherlands;* orcid.org/0000-0002-9446-9904

Piet D. Iedema − *Van't Hoff Institute for Molecular Sciences, University of Amsterdam, Amsterdam, The Netherlands;* orcid.org/0000-0003-1591-051X

Complete contact information is available at: https://pubs.acs.org/10.1021/acs.analchem.4c00938

Notes

The authors declare no competing financial interest.

■ ACKNOWLEDGMENTS

This material is based upon work supported by the National Science Foundation under Grant no. OISE 1743748. A.L. acknowledges funding from the Paris Ile-de-France Region—DIM Respore and DIM Matériaux anciens et patrimoniaux.

■ REFERENCES

(1) van den Berg, J. D. J. Analytical Chemical Studies on Traditional Oil Paints. Doctoral Thesis, University of Amsterdam, 2002.
(2) van den Berg, J. D.; Vermist, N. D.; Carlyle, L.; Holčapek, M.; Boon, J. J. *J. Sep. Sci.* **2004**, *27*, 181−199.
(3) de Viguerie, L.; Payard, P. A.; Portero, E.; Walter, Ph.; Cotte, M. *Prog. Org. Coat.* **2016**, *93*, 46−60.
(4) Wexler, H. *Chem. Rev.* **1964**, *64*, 591−611.
(5) Juita, D. B.; Dlugogorski, B. Z.; Kennedy, E. M.; Mackie, J. C. *Fire Sci. Rev.* **2012**, *1*, 3.
(6) Orlova, Y.; Harmon, R. E.; Broadbelt, L. J.; Iedema, P. D. *Prog. Org. Coat.* **2021**, *151*, 106041.
(7) Rahul, R.; Kitey, R. *Composites, Part B* **2016**, *85*, 336−342.
(8) Wang, D.; Klein, J.; Mejía, E. *Chem. Asian J.* **2017**, *12*, 1180−1197.
(9) Yeh, C. J.; Hu, M.; Shull, K. R. *Macromolecules* **2018**, *51*, 5511−5518.
(10) Chen, J.; Garcia, E. S.; Zimmerman, S. C. *Acc. Chem. Res.* **2020**, *53*, 1244−1256.
(11) Erhardt, D.; Tumosa, C. S.; Mecklenburg, M. F. *Stud. Conserv.* **2005**, *50*, 143−150.
(12) Bonaduce, I.; Carlyle, L.; Colombini, M. P.; Duce, C.; Ferrari, C.; Ribechini, E.; Selleri, P.; Tiné, M. R. *PLoS One* **2012**, *7*, No. e49333.
(13) Nardelli, F.; Martini, F.; Lee, J.; Lluvears-Tenorio, A.; La Nasa, J.; Duce, C.; Ormsby, B.; Geppi, M.; Bonaduce, I. *Sci. Rep.* **2021**, *11*, 14202.

(14) Pizzimenti, S.; Bernazzani, L.; Tinè, M. R.; Duce, C.; Bonaduce, I. *J. Therm. Anal. Calorim.* **2022**, *147*, 5451−5462.
(15) Lazzari, M.; Chiantore, O. *Polym. Degrad. Stab.* **1999**, *65*, 303−313.
(16) Vandenabeele, P.; Wehling, B.; Moens, L.; Edwards, H.; De Reu, M.; Van Hooydonk, G. *Anal. Chim. Acta* **2000**, *407*, 261−274.
(17) de Viguerie, L.; Ducouret, G.; Lequeux, F.; Moutard-Martin, T.; Walter, P. *C. R. Phys.* **2009**, *10*, 612−621.
(18) de Viguerie, L.; Jaber, M.; Pasco, H.; Lalevée, J.; Morlet-Savary, F.; Ducouret, G.; Rigaud, B.; Pouget, T.; Sanchez, C.; Walter, P. *Angew. Chem., Int. Ed.* **2017**, *56*, 1619−1623.
(19) de Viguerie, L.; Glanville, H.; Ducouret, G.; Jacquemot, P.; Dang, P. A.; Walter, P. *C. R. Phys.* **2018**, *19*, 543−552.
(20) Laporte, L.; Ducouret, G.; Gobeaux, F.; Lesaine, A.; Hotton, C.; Bizien, T.; Michot, L.; de Viguerie, L. *J. Colloid Interface Sci.* **2023**, *633*, 566−574.
(21) Ranquet, O.; Duce, C.; Bramanti, E.; Dietemann, P.; Bonaduce, I.; Willenbacher, N. *Nat. Commun.* **2023**, *14*, 1534.
(22) Mecklenburg, M. F.; Tumosa, C. S. *MRS Bull.* **2001**, *26*, 51−54.
(23) Mecklenburg, M. F.; Tumosa, C. S.; Erhardt, D. The Changing Mechanical Properties of Aging Oil Paints. *Materials Issues in Art and Archeology VII*; Materials Research Society: Warrendale, PA, 2004; pp 13−24.
(24) Ormsby, B.; Foster, G.; Learner, T.; Ritchie, S.; Schilling, M. *J. Therm. Anal. Calorim.* **2007**, *90*, 503−508.
(25) Ormsby, B.; Learner, T. J. S.; Foster, G. M.; Druzik, J. R.; Schilling, M. *Modern Paints Uncovered: Proceedings from the Modern Paints Uncovered Symposium*; Getty Conservation Institute: Los Angeles, 2007; pp 189−200.
(26) Phenix, A. *Thermal Mechanical Transitions in Artists' Oil Paints and Selected Conservation Materials: A Study by Dynamic Mechanical Analysis (DMA)*; The AIC Paintings Specialty Group: Los Angeles, 2009; pp 72−89.
(27) Salvant, J.; Barthel, E.; Menu, M. *Appl. Phys. A: Mater. Sci. Process.* **2011**, *104*, 509−515.
(28) Andersen, C. K.; Freeman, A.; Mortensen, M. N.; Beltran, V.; Łukomski, M.; Phenix, A. *Conservation of Modern Oil Paintings*; Springer, 2019; pp 403−417.
(29) Freeman, A.; Łukomski, M.; Beltran, V. *J. Am. Inst. Conserv.* **2020**, *59*, 27−39.
(30) Tiennot, M.; Paardekam, E.; Iannuzzi, D.; Hermens, E. *Sci. Rep.* **2020**, *10*, 7924.
(31) dePolo, G.; Walton, M.; Keune, K.; Shull, K. R. *Heritage Sci.* **2021**, *9*, 68.
(32) Marx, K. A. *Biomacromolecules* **2003**, *4*, 1099−1120.
(33) Johannsmann, D. *Phys. Chem. Chem. Phys.* **2008**, *10*, 4516.
(34) DeNolf, G. C.; Sturdy, L. F.; Shull, K. R. *Langmuir* **2014**, *30*, 9731−9740.
(35) Sturdy, L.; Casadio, F.; Kokkori, M.; Muir, K.; Shull, K. R. *Polym. Degrad. Stab.* **2014**, *107*, 348−355.
(36) Sturdy, L. F.; Yee, A.; Casadio, F.; Shull, K. R. *Polymer* **2016**, *103*, 387−396.
(37) Eaton, M. D.; Domene-López, D.; Wang, Q. G.; G Montalbán, M.; Martin-Gullon, I.; Shull, K. R. *Carbohydr. Polym.* **2021**, *261*, 117727.
(38) Chen, Y.; Shull, K. R. *Carbohydr. Polym. Technol. Appl.* **2023**, *5*, 100291.
(39) Martin, E. J.; Mathew, M. T.; Shull, K. R. *Langmuir* **2015**, *31*, 4008−4017.
(40) Sadman, K.; Wang, Q.; Chen, Y.; Keshavarz, B.; Jiang, Z.; Shull, K. R. *Macromolecules* **2017**, *50*, 9417−9426.
(41) Sadman, K.; Wiener, C. G.; Weiss, R. A.; White, C. C.; Shull, K. R.; Vogt, B. D. *Anal. Chem.* **2018**, *90*, 4079−4088.
(42) Bilchak, C. R.; Huang, Y.; Benicewicz, B. C.; Durning, C. J.; Kumar, S. K. *ACS Macro Lett.* **2019**, *8*, 294−298.
(43) Delgado, D. E.; Sturdy, L. F.; Burkhart, C. W.; Shull, K. R. *J. Polym. Sci., Part B: Polym. Phys.* **2019**, *57*, 1246−1254.
(44) dePolo, G. E.; Schafer, E.; Sadman, K.; Rivnay, J.; Shull, K. R. *J Vis Exp* **2020**, *155*, No. e60584.
(45) Sturdy, L. F.; Wright, M. S.; Yee, A.; Casadio, F.; Faber, K. T.; Shull, K. R. *Polymer* **2020**, *191*, 122222.
(46) Johannsmann, D. *The Quartz Crystal Microbalance in Soft Matter Research; Soft and Biological Matter*; Springer International Publishing: Cham, 2015; .
(47) Shull, K. R.; Taghon, M.; Wang, Q. *Biointerphases* **2020**, *15*, 021012.
(48) Baij, L.; Hermans, J. J.; Keune, K.; Iedema, P. D. *Macromolecules* **2018**, *51*, 7134−7144.
(49) Szántó, L.; Vogt, R.; Meier, J.; Auhl, D.; Van Ruymbeke, E.; Friedrich, C. *J. Rheol.* **2017**, *61*, 1023−1033.
(50) Ferry, J. *Viscoelastic Properties of Polymers*, 3rd ed.; John Wiley & Sons: New York, 1980.
(51) Chambon, F.; Winter, H. H. *J. Rheol.* **1987**, *31*, 683−697.
(52) Carlyle, L. *The Artist's Assistant: Oil Painting Instruction Manuals and Handbooks in Britain 1800−1900, with Reference to Selected Eighteenth-Century Sources*; Archetype Publication: London, 2001; .
(53) Cotte, M.; Checroun, E.; Susini, J.; Dumas, P.; Tchoreloff, P.; Besnard, M.; Walter, Ph. *Talanta* **2006**, *70*, 1136−1142.
(54) Kneepkens, I. *Understanding Historical Recipes for the Modification of Linseed Oil*; Master of Arts, University of Amsterdam: Amsterdam, 2012.
(55) O'Connell, P. A.; McKenna, G. B. *J. Chem. Phys.* **1999**, *110*, 11054−11060.

https://doi.org/10.1021/acs.analchem.4c00938
Anal. Chem. 2024, 96, 10551−10558